

High-order discontinuous Galerkin methods for solving the time-domain Maxwell equations on non-conforming simplicial meshes

Hassan Fahs

Ph.D. defense

Supervisor: Stéphane Lanteri

Co-supervisor: Francesca Rapetti

INRIA Sophia Antipolis

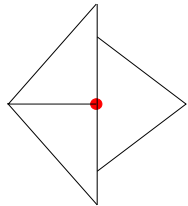
December 19, 2008

- Time-domain Maxwell's equations
 - Irregularly shaped geometries, heterogeneous media
 - Non-conforming, locally refined, triangular (2D)/tetrahedral (3D) meshes
- Discontinuous Galerkin (DG) methods: some generalities
 - Initially introduced to solve neutron transport problems (Reed and Hill, 1973)
 - Somewhere between finite element and finite volume methods, gathering many good features of both
 - Main properties
 - Can handle unstructured, non-conforming meshes
 - Can easily deal with discontinuous coefficients and solutions
 - Yield local finite element mass matrices
 - Naturally lead to discretization (h -) and interpolation order (p -) adaptivity
 - Can handle elements of various types and shapes
 - Amenable to efficient parallelization

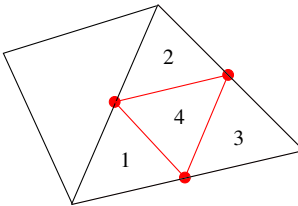
- Numerical ingredients (starting point to this study)
 - ☞ L. Fezoui, S. Lanteri, S. Lohrengel and S. Piperno: *ESAIM, M2AN*, 2005
 - Conforming discontinuous Galerkin time-domain (DGTD) method
 - Centered flux + explicit time integration
 - Nodal (Lagrange type) polynomial interpolation
- Overall objectives of this study
 - Investigate strengths and weaknesses of explicit DGTD methods using non-conforming simplicial meshes with arbitrary level hanging nodes
 - Theoretical and numerical aspects (stability, dispersion error, convergence)
 - Computational aspects

Context

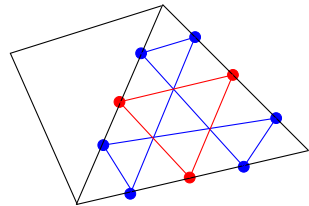
Non-conforming simplicial meshes



Non-conforming mesh



1-irregular mesh

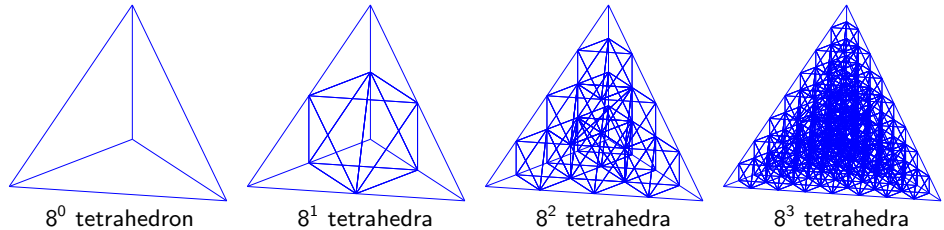


3-irregular mesh

- Red (non-conforming) refinement
 - Each triangle is split into 4 similar triangles
 - Each tetrahedron is split into 8 non-similar tetrahedra
- Can be used for more flexibility in the discretization of :
 - complex domains,
 - heterogeneous media.
- Expected to reduce memory consumption and computing time

Context

Non-conforming simplicial meshes



- Red (non-conforming) refinement
 - Each triangle is split into 4 similar triangles
 - Each tetrahedron is split into 8 non-similar tetrahedra
- Can be used for more flexibility in the discretization of :
 - complex domains,
 - heterogeneous media.
- Expected to reduce memory consumption and computing time

Content

- ① DGTD- \mathbb{P}_{p_i} method
 - Formulation (space and time discretizations)
 - Properties (stability, numerical dispersion)
- ② hp -like DGTD- $\mathbb{P}_{(p_1, p_2)}$ method
- ③ Numerical results in 2D and 3D
 - Numerical convergence
 - The general non-conforming mesh
 - Comparison with the conforming DGTD method
- ④ Arbitrary high-order leap-frog (LF_N) scheme
 - Properties (stability, convergence)
 - Numerical validation
- ⑤ Closure

DGTD- \mathbb{P}_{p_i} method

- Time-domain Maxwell's equations in $\Omega \subset \mathbb{R}^3$

$$\bar{\epsilon} \partial_t \vec{\mathbf{E}} - \operatorname{curl} \vec{\mathbf{H}} = 0 \quad \text{and} \quad \bar{\mu} \partial_t \vec{\mathbf{H}} + \operatorname{curl} \vec{\mathbf{E}} = 0$$

- Boundary conditions : $\partial\Omega = \Gamma_a \cup \Gamma_m$

$$\begin{cases} \vec{\mathbf{n}} \times \vec{\mathbf{E}} = 0 & \text{on } \Gamma_m \\ \vec{\mathbf{n}} \times \vec{\mathbf{E}} = -\sqrt{\frac{\mu}{\epsilon}} \vec{\mathbf{n}} \times (\vec{\mathbf{n}} \times \vec{\mathbf{H}}) & \text{on } \Gamma_a \end{cases}$$

- Triangulation of Ω : $\Omega_h = \bigcup \tau_i$

- Hanging nodes are allowed
- $a_{ik} = \tau_i \cap \tau_k$ (interface)
- $p = \{p_i : \tau_i \in \Omega_h\}$, p_i is the local polynomial degree
- Approximation space: $V_p(\Omega_h) := \{\mathbf{v} \in L^2(\Omega)^3 : \mathbf{v}|_{\tau_i} \in \mathbb{P}_{p_i}(\tau_i), \forall \tau_i \in \Omega_h\}$

DGTD- \mathbb{P}_{p_i} method

Space discretization

- Variational formulation: $\forall \vec{\varphi} \in \mathcal{P}_i = \text{Span}\{\vec{\varphi}_{ij}, 1 \leq j \leq d_i\}$

$$\left\{ \begin{array}{lcl} \int_{\tau_i} \vec{\varphi} \cdot \bar{\epsilon}_i \partial_t \vec{\mathbf{E}} & = & \int_{\tau_i} \text{curl } \vec{\varphi} \cdot \vec{\mathbf{H}} - \int_{\partial \tau_i} \vec{\varphi} \cdot (\vec{\mathbf{H}} \times \vec{\mathbf{n}}) \\ \int_{\tau_i} \vec{\varphi} \cdot \bar{\mu}_i \partial_t \vec{\mathbf{H}} & = & - \int_{\tau_i} \text{curl } \vec{\varphi} \cdot \vec{\mathbf{E}} + \int_{\partial \tau_i} \vec{\varphi} \cdot (\vec{\mathbf{E}} \times \vec{\mathbf{n}}) \end{array} \right.$$

- Centered fluxes [M. Remaki: *COMPEL*, 2000]

$$\vec{\mathbf{E}}|_{a_{ik}} = \frac{\vec{\mathbf{E}}_i + \vec{\mathbf{E}}_k}{2}, \quad \vec{\mathbf{H}}|_{a_{ik}} = \frac{\vec{\mathbf{H}}_i + \vec{\mathbf{H}}_k}{2} \quad (1)$$

- Replacing surface integrals using (1), and re-integrating by parts

$$\left\{ \begin{array}{lcl} \int_{\tau_i} \vec{\varphi} \cdot \bar{\epsilon}_i \partial_t \vec{\mathbf{E}}_i & = & \frac{1}{2} \int_{\tau_i} (\text{curl } \vec{\varphi} \cdot \vec{\mathbf{H}}_i + \text{curl } \vec{\mathbf{H}}_i \cdot \vec{\varphi}) - \frac{1}{2} \sum_{k \in \mathcal{V}_i} \int_{a_{ik}} \vec{\varphi} \cdot (\vec{\mathbf{H}}_k \times \vec{\mathbf{n}}_{ik}) \\ \int_{\tau_i} \vec{\varphi} \cdot \bar{\mu}_i \partial_t \vec{\mathbf{H}}_i & = & - \frac{1}{2} \int_{\tau_i} (\text{curl } \vec{\varphi} \cdot \vec{\mathbf{E}}_i + \text{curl } \vec{\mathbf{E}}_i \cdot \vec{\varphi}) + \frac{1}{2} \sum_{k \in \mathcal{V}_i} \int_{a_{ik}} \vec{\varphi} \cdot (\vec{\mathbf{E}}_k \times \vec{\mathbf{n}}_{ik}) \end{array} \right.$$

DGTD- \mathbb{P}_{p_i} method

- Matrix form of the space discretized DGTD- \mathbb{P}_{p_i} scheme :

$$\begin{cases} M_i^\epsilon \partial_t \mathbf{E}_i &= K_i \mathbf{H}_i - \sum_{k \in \mathcal{V}_i} S_{ik} \mathbf{H}_k \\ M_i^\mu \partial_t \mathbf{H}_i &= -K_i \mathbf{E}_i + \sum_{k \in \mathcal{V}_i} S_{ik} \mathbf{E}_k \end{cases}$$

- M_i^ϵ and M_i^μ are the symmetric positive definite mass matrices of size d_i
- K_i is the symmetric stiffness matrix of size d_i
- S_{ik} is the interface matrix of size $d_i \times d_k$:

$$(S_{ik})_{jl} = \frac{1}{2} \int_{a_{ik}} \vec{\varphi}_{ij} \cdot (\vec{\varphi}_{kl} \times \vec{n}_{ik})$$

- If a_{ik} is a conforming interface \Rightarrow no problem
- If a_{ik} is a non-conforming interface \Rightarrow we calculate S_{ik} using cubature formulas
 - 2D : Gauss-Legendre quadrature
 - 3D : Dunavant cubature formula

DGTD- \mathbb{P}_{p_i} method

Time discretization

- Second-order leap-frog (LF_2) time scheme
 - Unknowns related to \mathbf{E} are approximated at $t^n = n\Delta t$
 - Unknowns related to \mathbf{H} are approximated at $t^{n+\frac{1}{2}} = (n + \frac{1}{2})\Delta t$
- Matrix form of the space-time discretized DGTD- \mathbb{P}_{p_i} scheme :

$$\left\{ \begin{array}{lcl} M_i^\epsilon \frac{\mathbf{E}_i^{n+1} - \mathbf{E}_i^n}{\Delta t} & = & K_i \mathbf{H}_i - \sum_{k \in \mathcal{V}_i} S_{ik} \mathbf{H}_k \\ M_i^\mu \frac{\mathbf{H}_i^{n+3/2} - \mathbf{H}_i^{n+1/2}}{\Delta t} & = & -K_i \mathbf{E}_i + \sum_{k \in \mathcal{V}_i} S_{ik} \mathbf{E}_k \end{array} \right.$$

Properties of the DGTD- \mathbb{P}_{p_i} method

Stability

- Local discrete electromagnetic energy

$$\mathcal{E}_i^n = \frac{1}{2} ({}^t \mathbf{E}_i^n M_i^\epsilon \mathbf{E}_i^n + {}^t \mathbf{H}_i^{n-\frac{1}{2}} M_i^\mu \mathbf{H}_i^{n+\frac{1}{2}})$$

- The energy \mathcal{E}_i^n is exactly conserved (when $\Gamma_a = \emptyset$)
- The DGTD- \mathbb{P}_{p_i} method is stable if

$$\forall i, \forall k \in \mathcal{V}_i, \quad c_i \Delta t [2\alpha_i + \beta_{ik}] < \frac{4V_i}{P_i}$$

- The dimensionless constants α_i and β_{ik} ($k \in \mathcal{V}_i$) verify

$$\forall \vec{\mathbf{X}} \in \mathcal{P}_i, \quad \|\operatorname{curl} \vec{\mathbf{X}}\|_{\tau_i} \leq \frac{\alpha_i P_i}{V_i} \|\vec{\mathbf{X}}\|_{\tau_i} \quad \text{and} \quad \|\vec{\mathbf{X}}\|_{a_{ik}}^2 \leq \frac{\beta_{ik} S_{ik}}{V_i} \|\vec{\mathbf{X}}\|_{\tau_i}^2$$

- Numerical CFL values for the DGTD- \mathbb{P}_p method

p	0	1	2	3	4	5	6	7	8	9	10
CFL(LF ₂)	1.0	0.3	0.2	0.1	0.08	0.06	0.045	0.035	0.03	0.025	0.02

Properties of the DGTD- \mathbb{P}_{p_i} method

Numerical dispersion

☞ D. Sármány, M. Botchev and J. van der Vegt : *J. Sci. Comput.*, 2007

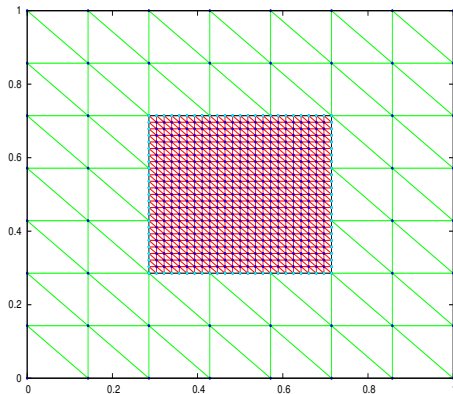
- Two-dimensional Maxwell's equation (TMz)

$$\begin{cases} \epsilon \partial_t E_z - \partial_x H_y + \partial_y H_x = 0 \\ \mu \partial_t H_x + \partial_y E_z = 0 \\ \mu \partial_t H_y - \partial_x E_z = 0 \end{cases}$$

- Eigenmode in a unitary PEC square cavity
 - Frequency=212 MHz
 - $p_i = p$ is uniform
 - Simulations are carried out for time $t = 60$ (43 periods)
- 7-irregular non-conforming meshes (**a centered zone is refined 3 times**)
 - For $p = 0, 1 \Rightarrow 10$ points per wavelength
 - For $p = 2, 3, 4 \Rightarrow 6$ points per wavelength

Eigenmode in a PEC cavity

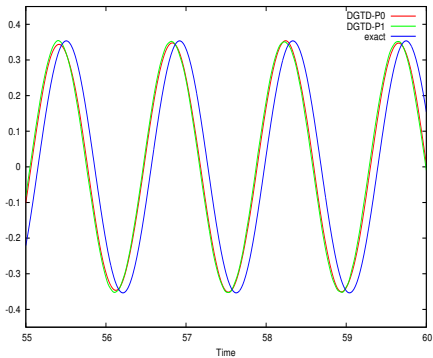
Non-conforming mesh



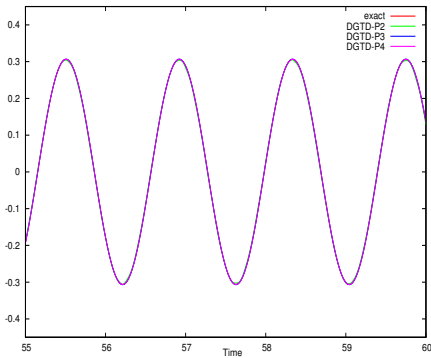
The centered zone is locally refined 3 times
7-irregular mesh

Numerical dispersion

DGTD- \mathbb{P}_p , $p \leq 1$ method



DGTD- \mathbb{P}_p , $p \geq 2$ method



DGTD- \mathbb{P}_p method : time evolution of the H_x component
Zoom on the last 5 periods

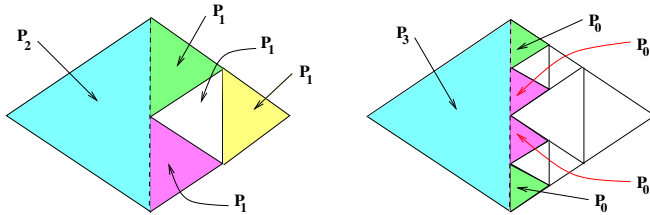
hp -like DGTD- $\mathbb{P}_{(p_1,p_2)}$ method

- H. Fahs et al. : *IEEE Trans. Magn.*, 2008
- H. Fahs : *Int. J. Numer. Anal. Model.*, 2008, to appear

- The DGTD- $\mathbb{P}_{(p_1,p_2)}$ method involves:
 - high polynomial degrees " p_1 " in the coarse elements,
 - low polynomial degrees " p_2 " in the refined elements.
- The DGTD- $\mathbb{P}_{(p_1,p_2)}$ method is stable under a CFL-like condition

$$\text{CFL}(\text{DGTD-}\mathbb{P}_{(p_1,p_2)}) = \text{CFL}(\text{DGTD-}\mathbb{P}_{p_2})$$

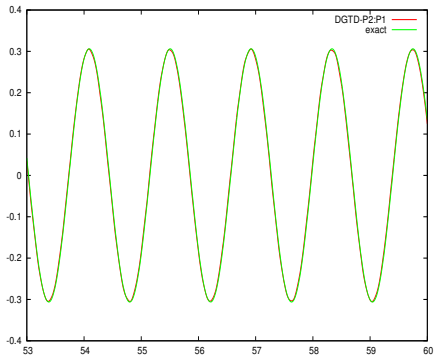
→ $\text{CFL}(\text{DGTD-}\mathbb{P}_{(2,1)}) = \text{CFL}(\text{DGTD-}\mathbb{P}_1) = 0.3$



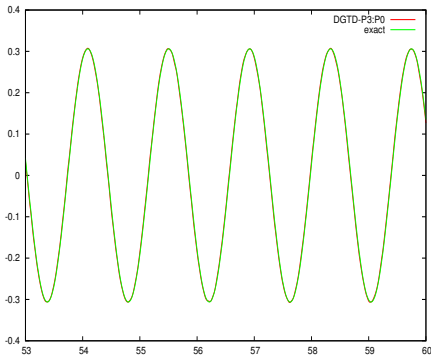
DGTD- $\mathbb{P}_{(p_1, p_2)}$ method

Eigenmode in a PEC cavity

DGTD- $\mathbb{P}_{(2,1)}$ method



DGTD- $\mathbb{P}_{(3,0)}$ method



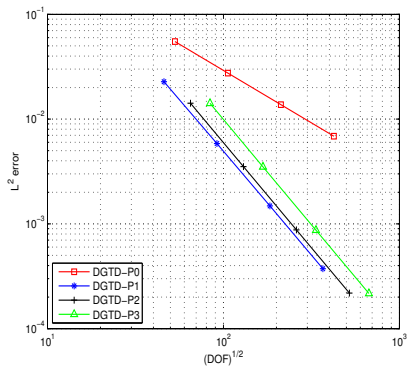
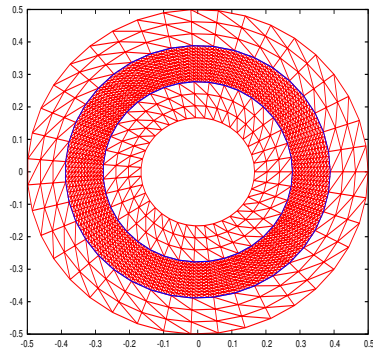
DGTD- $\mathbb{P}_{(p_1, p_2)}$ method : time evolution of the H_x component
Zoom on the last 5 periods

Numerical results

- Homogeneous media
 - ① eigenmode in a PEC cavity (in 2D & 3D)
 - ② concentric PEC cylinders resonator
 - ③ circular PEC resonator
 - ④ wedge-shaped PEC resonator
- Heterogeneous media
 - ① rectangular PEC resonator with one material interface
 - ② dielectric in a PEC cavity with two material interfaces
 - ③ dielectric cylinder illuminated by a plane wave
 - ④ scattering by multilayered dielectric cylinder
 - ⑤ propagation in a heterogeneous human head model

Concentric PEC cylinders resonator

Convergence study: homogeneous case



Numerical convergence of the DGTD- \mathbb{P}_p method

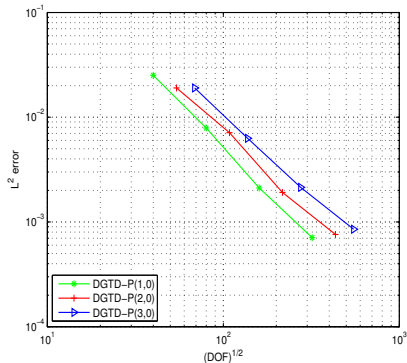
Global (space and time) L^2 error versus the square root of # DOF

Slopes: 1.0 (DGTD- \mathbb{P}_0 method) and 2.0 (DGTD- \mathbb{P}_p , $p \geq 1$ method)

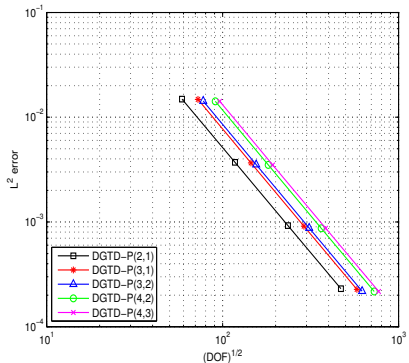
Concentric PEC cylinders resonator

Convergence study: homogeneous case

DGTD- $\mathbb{P}_{(p_1, p_2)}$ method, $p_2 = 0$



DGTD- $\mathbb{P}_{(p_1, p_2)}$ method, $p_2 \neq 0$



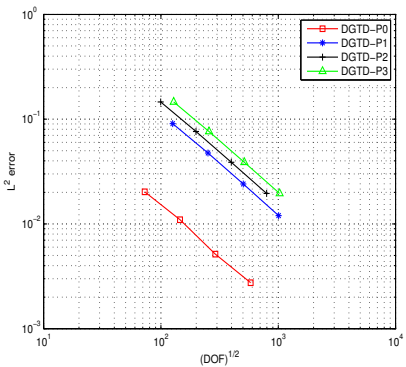
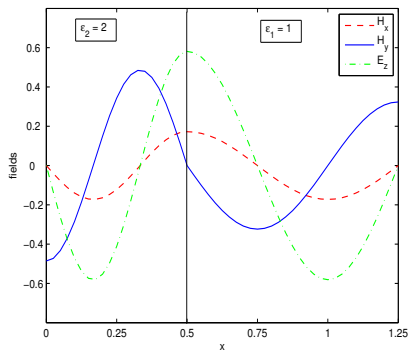
Numerical convergence of the DGTD- $\mathbb{P}_{(p_1, p_2)}$ method

Global (space and time) L^2 error versus the square root of # DOF

Slopes: 1.5 (for $p_2 = 0$) and 2.0 (for $p_2 \neq 0$)

Rectangular PEC resonator with one material interface

Convergence study: heterogeneous case



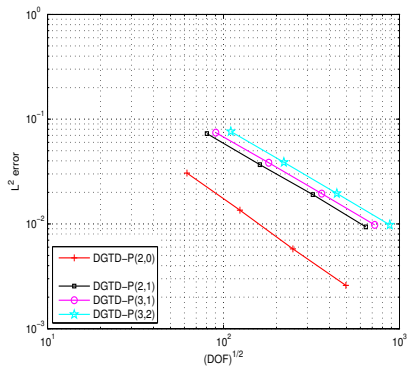
Numerical convergence of the DGTD-P_p method

Global (space and time) L^2 error versus the square root of # DOF

Slopes: 1.0 $\forall p$

Rectangular PEC resonator with one material interface

Convergence study: heterogeneous case



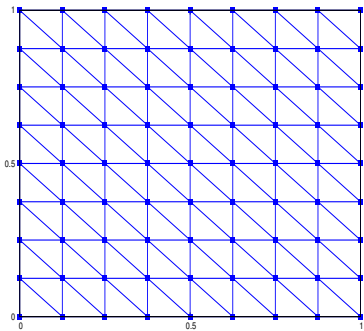
Numerical convergence of the DGTD- $\mathbb{P}_{(p_1, p_2)}$ method
Global (space and time) L^2 error versus the square root of # DOF

Slopes: 1.2 $\forall p_1, \forall p_2$

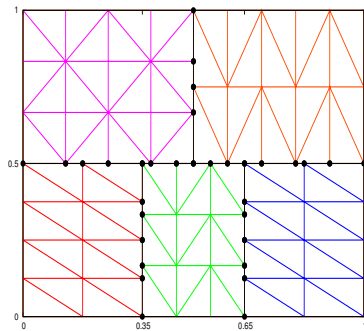
Eigenmode in a PEC cavity : the 2D case

General non-conforming mesh

Regular conforming mesh
81 nodes & 128 triangles
& 208 faces



General non-conforming mesh
76 nodes (32 hanging nodes)
& 94 triangles & 169 faces



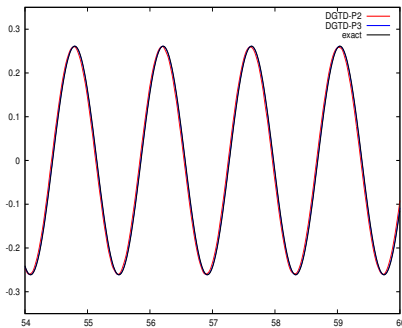
	\mathbb{P}_2	\mathbb{P}_3	\mathbb{P}_4
Error	3.7E-02	8.6E-03	5.5E-03
# DOF	768	1280	1920
CPU time	5.5	18	37

	\mathbb{P}_2	\mathbb{P}_3	\mathbb{P}_4
Error	3.5E-02	8.1E-03	5.2E-03
# DOF	564	940	1410
CPU time	5	15	31

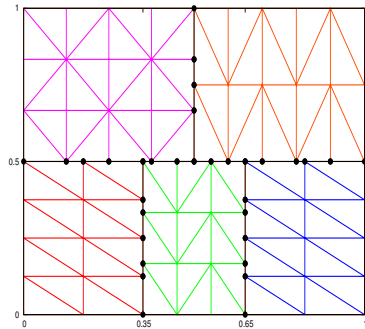
Eigenmode in a PEC cavity : the 2D case

General non-conforming mesh

Time evolution of E_z
Zoom on the last 4/43 periods
DGTD- \mathbb{P}_2 /DGTD- \mathbb{P}_3 /exact



General non-conforming mesh
76 nodes (32 hanging nodes)
& 94 triangles & 169 faces



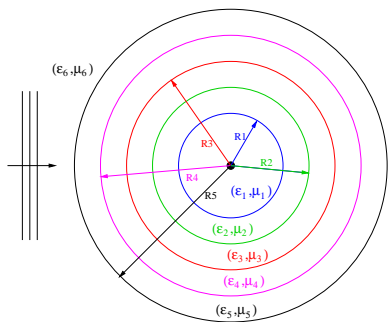
	\mathbb{P}_2	\mathbb{P}_3	\mathbb{P}_4
Error	3.7E-02	8.6E-03	5.5E-03
# DOF	768	1280	1920
CPU time	5.5	18	37

	\mathbb{P}_2	\mathbb{P}_3	\mathbb{P}_4
Error	3.5E-02	8.1E-03	5.2E-03
# DOF	564	940	1410
CPU time	5	15	31

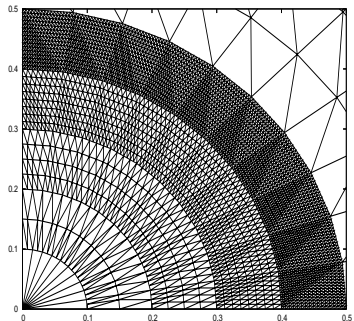
Scattering by multilayered dielectric cylinder

Comparison conforming/non-conforming methods

Computational domain



(15-irregular) Non-conforming mesh

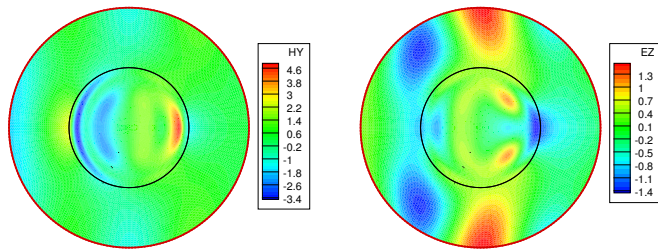


Region	Region 1	Region 2	Region 3	Region 4	Region 5	Region 6
Interpolation order	p_1	p_2	p_3	p_4	p_5	p_6
Level of refinement	0	1	2	3	4	0
# triangles non-conforming mesh	40	320	1280	5120	20480	400

Scattering by multilayered dielectric cylinders

Reference solution

Contour lines at time $t = 5$



- Ω is a cylinder of radius one
- First order Silver-Müller ABC at the artificial boundary
- Reference solution is constructed in a very fine conforming mesh using DGTD- \mathbb{P}_4 method

# nodes	# triangles	# DOF
25001	49750	746250

Scattering by multilayered dielectric cylinders

DGTD- \mathbb{P}_p method: conforming mesh

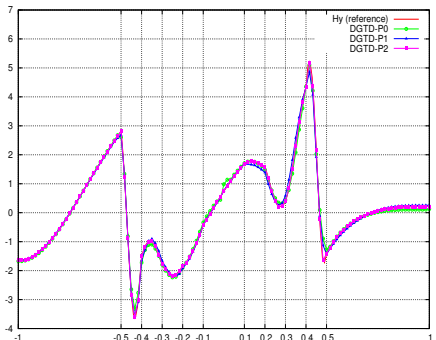
DGTD- \mathbb{P}_p	Error on H_y	CPU (min)	# DOF
DGTD- \mathbb{P}_0	8.6 %	25	28560
DGTD- \mathbb{P}_1	7.6 %	137	85680
DGTD- \mathbb{P}_2	2.2 %	286	171360
DGTD- \mathbb{P}_3	2.2 %	842	285600

hp-like DGTD method: non-conforming mesh

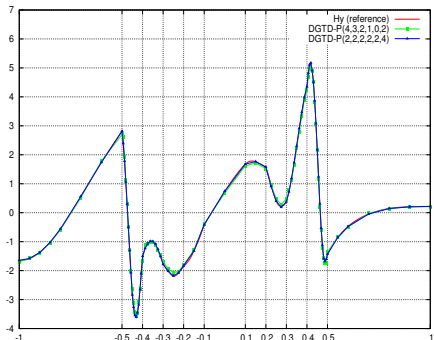
DGTD- $\mathbb{P}_{(p_1, p_2, p_3, p_4, p_5, p_6)}$	Error on H_y	CPU (min)	# DOF
DGTD- $\mathbb{P}_{(4,3,2,1,0,2)}$	5.0 %	12	49720
DGTD- $\mathbb{P}_{(4,3,2,2,0,2)}$	4.8 %	13	65080
DGTD- $\mathbb{P}_{(4,3,2,2,1,4)}$	3.5 %	17	109640
DGTD- $\mathbb{P}_{(4,2,2,4,1,4)}$	3.2 %	21	154440
DGTD- $\mathbb{P}_{(2,2,2,2,2,4)}$	2.5 %	20	169440

Scattering by multilayered dielectric cylinders

DGTD- \mathbb{P}_p method
Conforming mesh



hp-like DGTD method
Non-conforming mesh

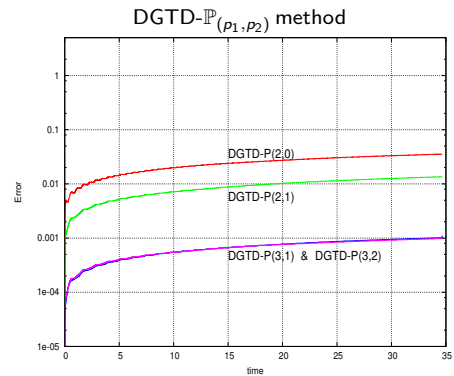
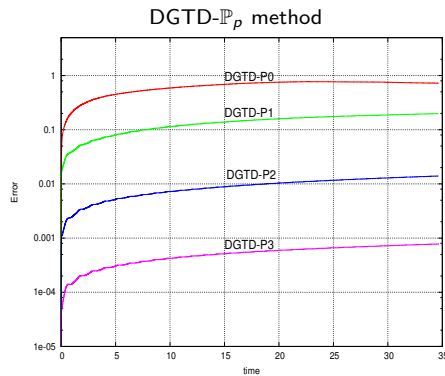


1D distribution of H_y along $y = 0.0$ at time $t = 5$

Eigenmode in a PEC cavity : the 3D case

Comparison conforming/non-conforming methods

- Frequency = 256 MHz
- Unstructured mesh: 4406 tetrahedra, 962 nodes & 9235 faces
- Degree p_2 is used in 1434 tetrahedra (1905 non-conforming interfaces)



Time evolution of the L^2 error for time $t = 35$ (30 periods)

Eigenmode in a PEC cavity : the 3D case

Comparison conforming/non-conforming methods

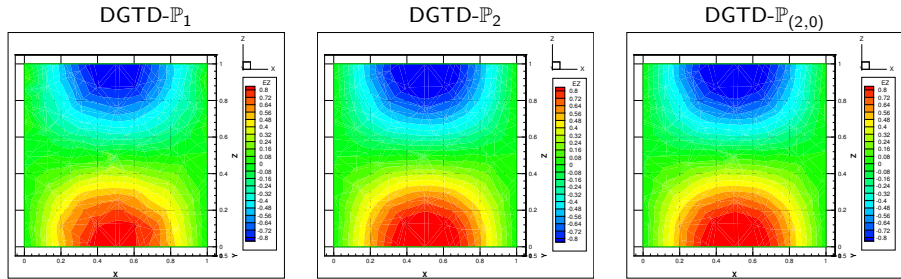


Figure: Contour lines of E_z in the plane $y = 0.5$

DGTD- \mathbb{P}_p	DGTD- \mathbb{P}_0	DGTD- \mathbb{P}_1	DGTD- \mathbb{P}_2	DGTD- \mathbb{P}_3
L^2 error	7.2E-01	2.0E-01	1.4E-02	8.0E-04
CPU time (min)	4	40	213	859
DGTD- $\mathbb{P}_{(p_1,p_2)}$	DGTD- $\mathbb{P}_{(2,0)}$	DGTD- $\mathbb{P}_{(2,1)}$	DGTD- $\mathbb{P}_{(3,1)}$	DGTD- $\mathbb{P}_{(3,2)}$
L^2 error	3.6E-02	1.3E-02	1.0E-03	8.8E-04
CPU time (min)	35	106	260	499

Propagation in a heterogeneous human head model

Comparison conforming/non-conforming methods

- Dipole source type

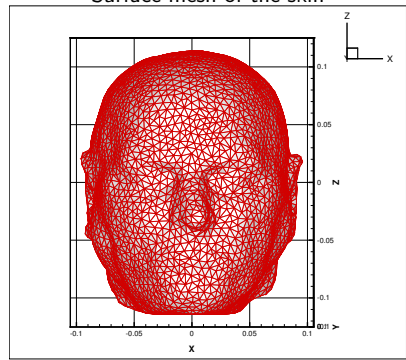
$$J_z(\mathbf{x}, t) = z_0 \delta(\mathbf{x} - \mathbf{x}_d) f(t) \quad \text{and} \quad f(t) = \sin \omega t$$

- Source is localized near the right ear of the head
- Frequency = 1800 MHz

Electromagnetic characteristics
of the selected head tissues

Tissue	ϵ_r	σ	ρ
Brain	43.55	1.15	1050.0
CSF	67.20	2.92	1000.0
Skull	15.56	0.43	1200.0
Skin (wet)	43.85	1.23	1100.0

Surface mesh of the skin



Propagation in a heterogeneous human head model

Comparison conforming/non-conforming methods

Contour lines of the DFT of E_z

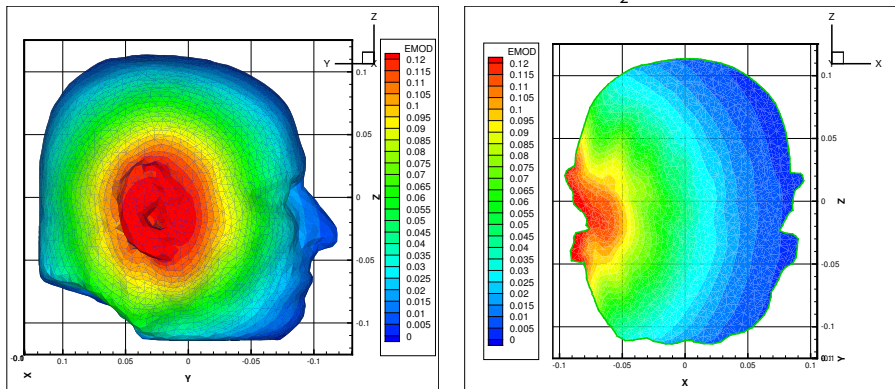


Table: CPU time in hours

Method	DGTD- \mathbb{P}_1	DGTD- \mathbb{P}_2	DGTD- \mathbb{P}_3	DGTD- $\mathbb{P}_{(2,1)}$
CPU time	6 h	30 h	87 h	12 h

Arbitrary high-order time scheme

- H. Spachmann, R. Schuhmann and T. Weiland : *Int. J. Numer. Model.*, 2002
- J.L. Young : *Radio Science*, 2001

- High-order leap-frog (LF_N) time scheme

$$\left\{ \begin{array}{l} \mathbf{T}_1 = \Delta t(M_i^\epsilon)^{-1} \operatorname{curl}_h \vec{\mathbf{H}}_i^{n+\frac{1}{2}}, \quad \mathbf{T}_1^* = -\Delta t(M_i^\mu)^{-1} \operatorname{curl}_h \vec{\mathbf{E}}_i^{n+1} \\ \mathbf{T}_2 = -\Delta t(M_i^\mu)^{-1} \operatorname{curl}_h \mathbf{T}_1, \quad \mathbf{T}_2^* = \Delta t(M_i^\epsilon)^{-1} \operatorname{curl}_h \mathbf{T}_1^* \\ \mathbf{T}_3 = \Delta t(M_i^\epsilon)^{-1} \operatorname{curl}_h \mathbf{T}_2, \quad \mathbf{T}_3^* = -\Delta t(M_i^\mu)^{-1} \operatorname{curl}_h \mathbf{T}_2^* \end{array} \right.$$

$$\text{LF}_2 : \left\{ \begin{array}{lcl} \mathbf{E}_i^{n+1} & = & \mathbf{E}_i^n + \mathbf{T}_1 \\ \mathbf{H}_i^{n+\frac{3}{2}} & = & \mathbf{H}_i^{n+\frac{1}{2}} + \mathbf{T}_1^* \end{array} \right.$$

$$\text{LF}_4 : \left\{ \begin{array}{lcl} \mathbf{E}_i^{n+1} & = & \mathbf{E}_i^n + \mathbf{T}_1 + \mathbf{T}_3/24 \\ \mathbf{H}_i^{n+\frac{3}{2}} & = & \mathbf{H}_i^{n+\frac{1}{2}} + \mathbf{T}_1^* + \mathbf{T}_3^*/24 \end{array} \right.$$

→ The LF_4 scheme requires twice more memory storage and 3 times more arithmetic operations than the LF_2 scheme

LF_N based DGTD- \mathbb{P}_{p_i} method

General form

- General form of the LF_N based DGTD- \mathbb{P}_{p_i} method :

$$\begin{cases} \mathbb{M}^\epsilon \frac{\mathbb{E}^{n+1} - \mathbb{E}^n}{\Delta t} = \mathbb{S}_N \mathbb{H}^{n+\frac{1}{2}} \\ \mathbb{M}^\mu \frac{\mathbb{H}^{n+\frac{3}{2}} - \mathbb{H}^{n+\frac{1}{2}}}{\Delta t} = -{}^t \mathbb{S}_N \mathbb{E}^{n+1} \end{cases}$$

where the $d \times d$ matrix \mathbb{S}_N verifies:

$$\mathbb{S}_N = \begin{cases} \mathbb{S} & \text{if } N = 2 \\ \mathbb{S}(\mathbb{I} - \frac{\Delta t^2}{24} \mathbb{M}^{-\mu} {}^t \mathbb{S} \mathbb{M}^{-\epsilon} \mathbb{S}) & \text{if } N = 4 \end{cases}$$

- \mathbb{E} and \mathbb{H} are of size $d = \sum_i d_i$
- \mathbb{M}^ϵ and \mathbb{M}^μ are block diagonal mass matrices of size d with diagonal blocks equal to M_i^ϵ and M_i^μ respectively

Properties of the LF_N based DGTD- \mathbb{P}_{p_i} method

Stability

☞ H. Fahs and S. Lanteri: *J. Comput. Appl. Math.*, 2008, submitted

- Global discrete electromagnetic energy:

$$\mathcal{E}^n = \frac{1}{2} \left({}^t \mathbb{E}^n \mathbb{M}^\epsilon \mathbb{E}^n + {}^t \mathbb{H}^{n-\frac{1}{2}} \mathbb{M}^\mu \mathbb{H}^{n+\frac{1}{2}} \right)$$

- The energy \mathcal{E}^n is exactly conserved (when $\Gamma_a = \emptyset$)
- The LF_N based DGTD- \mathbb{P}_{p_i} method is stable if

$$\Delta t \leq \frac{2}{d_N} \quad \text{with} \quad d_N = \|\mathbb{M}^{-\frac{\mu}{2}} {}^t \mathbb{S}_N \mathbb{M}^{-\frac{\epsilon}{2}}\|$$

☞ $\nu_N = \text{CFL}(\text{LF}_N)/\text{CFL}(\text{LF}_2)$

N	2	4	6	8	10	12	14	16	18	20
ν_N	1.0	2.85	3.68	3.79	5.27	4.44	6.42	7.53	7.27	8.91

Properties of the LF_N based DGTD- \mathbb{P}_{p_i} method

Convergence

☞ J.S. Hesthaven and T. Warburton: *J. Comput. Phys.*, 2002

- ✖ Exact solution : $\vec{\mathbf{U}}(t) = (\vec{\mathbf{E}}(t), \vec{\mathbf{H}}(t)) \in \mathbf{H}^s(\tau_i) \times \mathbf{H}^s(\tau_i)$
- ✖ Numerical solution : $\vec{\mathbf{U}}_h(t) = (\vec{\mathbf{E}}_h(t), \vec{\mathbf{H}}_h(t)) \in V_p(\Omega_h) \times V_p(\Omega_h)$

- Convergence:

$$\|\vec{\mathbf{U}} - \vec{\mathbf{U}}_h\|_{0,\Omega} \leq C \left(\frac{h^\nu}{p^s} + T \frac{h^{\nu-1}}{p^{s-\frac{3}{2}}} \right) \max_{t \in [0, T]} \|\vec{\mathbf{U}}(t)\|_{s,\Omega}$$

- Convergence of the divergence error:

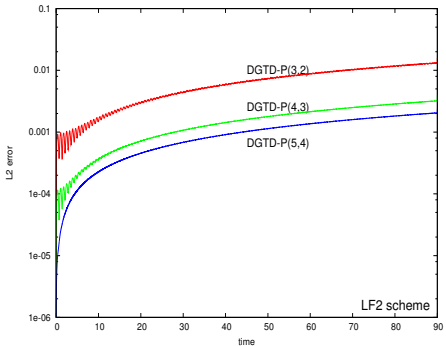
$$\|\nabla \cdot (\vec{\mathbf{U}} - \vec{\mathbf{U}}_h)\|_{0,\Omega} \leq C \left(\frac{h^{\nu-1}}{p^{s-1}} + T \frac{h^{\nu-2}}{p^{s-\frac{7}{2}}} \right) \max_{t \in [0, T]} \|\vec{\mathbf{U}}(t)\|_{s,\Omega}$$

- $\nu = \min\{s, p+1\}$
- $C(\epsilon, \mu)$ independent of h and p

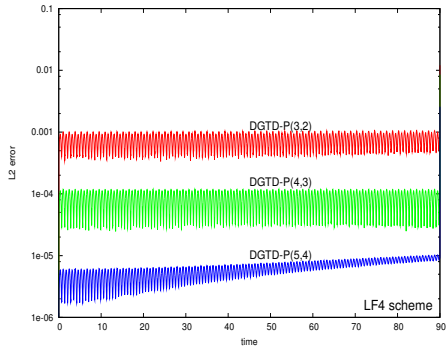
Eigenmode in a PEC cavity: the 2D case

- Comparison between LF_2/LF_4 based DGTD- $\mathbb{P}_{(p_1, p_2)}$ method
- Non-conforming mesh: 152 triangles (128 in the refined region)
97 nodes (24 hanging nodes)

LF_2 based DGTD- $\mathbb{P}_{(p_1, p_2)}$ method



LF_4 based DGTD- $\mathbb{P}_{(p_1, p_2)}$ method



Time evolution of the L^2 error for time $t = 90$ (65 periods)

Eigenmode in a PEC cavity: the 2D case

Comparison between LF_2/LF_4 based DGTD- $\mathbb{P}_{(p_1,p_2)}$ method

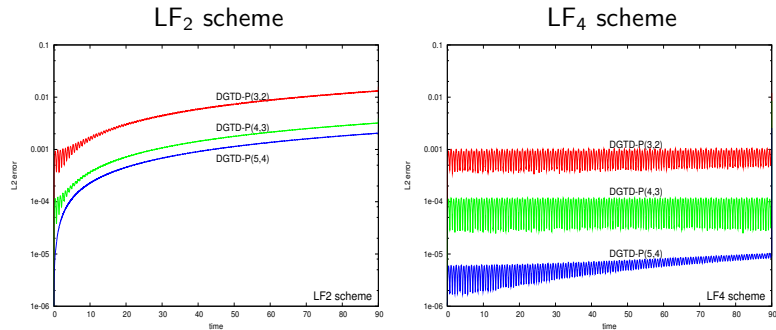


Table: L^2 -error, CPU time in seconds and # DOF to reach time $t = 90$

DGTD- $\mathbb{P}_{(p_1,p_2)}$	# DOF	LF ₂ scheme		LF ₄ scheme	
		Error	CPU time	Error	CPU time
DGTD- $\mathbb{P}_{(3,2)}$	1008	1.3E-02	29 s	8.6E-04	20 s
DGTD- $\mathbb{P}_{(4,3)}$	1640	3.2E-03	86 s	9.6E-05	60 s
DGTD- $\mathbb{P}_{(5,4)}$	2424	2.0E-03	183 s	9.4E-06	125 s

h -convergence of the DGTD- $\mathbb{P}_{(p_1, p_2)}$ method

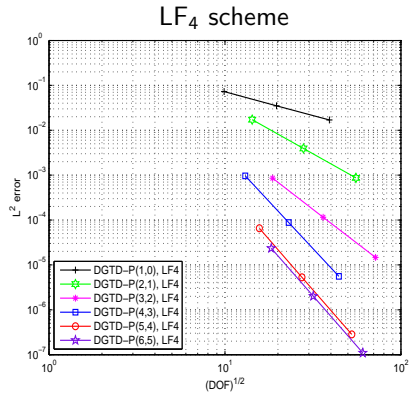
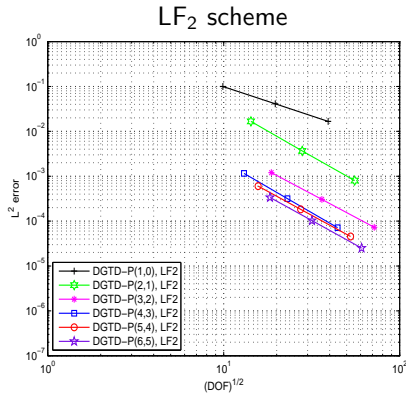
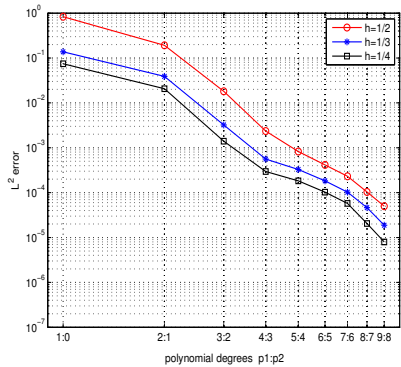


Table: Asymptotic h -convergence orders

(p_1, p_2)	(1,0)	(2,1)	(3,2)	(4,3)	(5,4)	(6,5)
LF ₂	1.30	2.23	2.08	2.27	2.13	2.17
LF ₄	1.05	2.20	3.01	4.21	4.50	4.48

p -convergence of the DGTD- $\mathbb{P}_{(p_1, p_2)}$ method

LF₂ scheme



LF₄ scheme

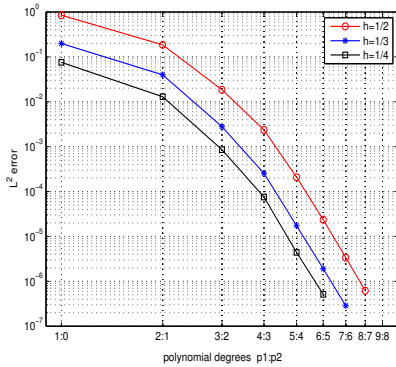


Table: p -convergence for $h = 1/3$

(p_1, p_2)	(1,0)	(2,1)	(3,2)	(4,3)	(5,4)	(6,5)	(7,6)
LF ₂	1.3E-01	3.9E-02	3.2E-03	5.6E-04	3.2E-04	1.8E-04	1.0E-04
LF ₄	1.9E-01	3.9E-02	2.7E-03	2.5E-04	1.7E-05	1.9E-06	2.6E-07

Concluding remarks

- Discontinuous Galerkin time-domain
 - can handle non-conforming meshes with arbitrary level hanging nodes,
 - the interpolation order may vary from element to element in the mesh,
 - stability is proved theoretically and the dispersion error is studied numerically.
- Numerical experiments
 - the convergence order is bounded by 2 (homogeneous media) and by 1 (heterogeneous media),
 - the general non-conforming mesh does not affect on the quality of the solution,
 - compared with the conforming DGTD method, the hp -like method can lead to notable reductions in the CPU time and memory consumption.
- High-order leap-frog (LF_N) based DGTD method
 - properties (stability, hp *a priori* estimates),
 - the LF_4 scheme is more accurate and requires less CPU than the LF_2 scheme,
 - spectral convergence with the LF_4 scheme.

Future works

- Design of a *hp*-adaptive DGTD method:
 - *a posteriori* error estimator,
 - hierarchical basis functions.
- Improvement of the efficiency of the *hp*-like method:
 - local time stepping,
 - ☞ S. Piperno: *M2AN*, 2006
 - hybrid explicit/implicit scheme.
 - ☞ Research activities of Nachos project-team
- Convergence properties for irregular solution (heterogeneous media):
 - regularization techniques,
 - ☞ E. Kashdan and E. Turkel: *J. Comput. Phys.*, 2006
 - hybrid centered/upwinding scheme.
 - ☞ W. Cai and S. Deng: *J. Comput. Phys.*, 2003
- High-order absorbing boundary conditions